machines

Article

An Air Spring Resonant Vibration Exciter for Large Structures

Renato Brancati [1], Domenico De Falco [2], Giandomenico Di Massa [1], Stefano Pagano [1,*] and Ernesto Rocca [1]

[1] Dipartimento di Ingegneria Industriale, Università di Napoli Federico II, 80125 Napoli, Italy; renato.brancati@unina.it (R.B.); giandomenico.dimassa@unina.it (G.D.M.); ernesto.rocca@unina.it (E.R.)
[2] Dipartimento di Ingegneria, Università degli Studi della Campania "Luigi Vanvitelli", 81100 Caserta, Italy; domenico.defalco@unicampania.it
* Correspondence: stefano.pagano@unina.it

Abstract: Periodic monitoring of large industrial and civil structures is carried out through static and dynamic measurements. The monitoring, carried out over many years, offers important information for evaluating the health of structures and their management. Dynamic tests are carried out starting from measurements of the vibrations of the structure induced by mechanical devices or by the surrounding environment. If a ground support element is available, it is possible to exert a forcing action on the structure using actuators fixed to the support. When a ground support is unavailable, the structure can be forced using devices comprised of masses with rotary or reciprocating translational motion. These masses must be large enough to excite appreciable mechanical vibrations of the structure. In this paper, a vibration exciter, based on a mass suspended on an air spring and forced to vibrate at the resonant frequency, is proposed. Thanks to the resonant condition, the force transmitted to the structure is amplified compared to that applied to the mass. The excitation frequency can be adjusted by altering the inflation pressure of the air spring to modify the natural frequency of the system. In the paper, after the presentation of some mechanical devices used as vibration exciters for large structures, the proposed device is described and the first experimental results are reported.

Keywords: periodic monitoring; vibration exciters; air springs; structural health monitoring (SHM); bridges

Citation: Brancati, R.; De Falco, D.; Di Massa, G.; Pagano, S.; Rocca, E. An Air Spring Resonant Vibration Exciter for Large Structures. *Machines* **2024**, *12*, 131. https://doi.org/10.3390/machines12020131

Received: 7 December 2023
Revised: 6 February 2024
Accepted: 10 February 2024
Published: 12 February 2024

1. Introduction

Monitoring of large constructions with high safety and durability requirements, such as bridges, tall buildings, bulkheads, tunnels, silos, chimneys, offshore platforms, is performed with the aim of verifying the hypotheses of the design, the calibration of an FEM model, the update of the technical specifications, as well as to evaluate the health of the structures, to detect the presence of any damage, to locate it, and to quantify its severity [1,2].

For example, with reference to road and railway bridges, periodic monitoring operations consist of a preliminary visual inspection of all the parts of the structure, sometimes with the aid of drones to closely observe the less accessible parts, to locate the external state of degradation of the materials. For a more in-depth knowledge of the state of the structure, it is possible to use a monitoring system based on the use of sensors, capable of highlighting a variation in the characteristics of the structure. The reduction in the performance of a structure is mainly caused by the degradation of the materials due to atmospheric agents and variations in load conditions.

The use of a monitoring system makes it possible to evaluate the performance of a structure over time and to plan maintenance works with objective criteria, limiting the progression of deterioration and thus lengthening the operational life of the structure. Therefore, it would be advisable, within economic and logistic limits, to monitor the health of a facility throughout its life by periodically detecting certain quantities and comparing them with those deducible from the corresponding theoretical model. In the case of new structures, the first tests are often performed before the structure comes into operation to have an initial reference [3]. The continuous reduction of the costs of monitoring systems allows new and existing structures to be observed [4]. However, it must be taken into account that the dynamics of the structure is not only influenced by its degradation but also by other factors, such as temperature variations, that make the identification of damage more difficult [5,6].

IoT technology, through low-cost self-powered sensors, enables the detection of structural vibrations, allowing the identification of parameters that define the health of a structure [7]. In [8], several novel methods linking vibration-based damage detection techniques with machine learning are documented.

In this context, diagnostic techniques that use computer vision measurements become of considerable interest [9,10]. In [11], a review of the computer vision techniques adopted and under study are reported. It shows that this technique allows the performance of analyses both at a local level (to highlight crack, spalling, delamination, rust, and loose bolt detection phenomena) and at a global level (for displacement measurements, for the analysis of structural behaviour, for modal identification, etc.)

Static and dynamic monitoring are two approaches used for the assessment and maintenance of structures; the first one involves the measurement and the analysis of static or quasi-static response of the structure to assess its behavior and detect any changes or abnormalities. Dynamic monitoring involves the acquisition of signals from sensors and their processing to obtain useful parameters for evaluating the performance of the structure; the data must be archived so that they can be compared with pre-existing data and with those that will be detected to capture and to analyze the dynamic response of the structures to external excitations as well as to identify dynamic parameters (natural frequencies, mode shapes, damping characteristics), dynamic amplification, forces in bearings, crack opening changes, etc.

These parameters can be identified through the knowledge of the input excitation and of the output signals detected by the sensors. Dynamic monitoring requires the structure to be excited in order to vibrate. In the case of large dimensions, structures are normally excited in the following ways:

a. By inducing a free response of the structure by applying an impulse excitation provided by an impact force or by suddenly releasing a load [12,13]. For example (Figure 1), free vibration may be generated by means of impulsive excitation due to a truck going down a step to excite a bridge or by suddenly releasing the force exerted by a tugboat on an offshore structure. In [14], an interesting loading hammer is presented. It comprises a mass raised by an electric motor to a predetermined height. Upon reaching this height, the mass is disengaged from the electric motor through an electromagnetic clutch and released onto the structure below. A sensor detects the movement of the mass and, promptly after impact, a brake engages to inhibit any rebound off the structure.
b. By adopting a vibration exciter, i.e., a device able to provide a harmonic force, such as actuators, shakers, counter-rotating unbalanced discs, etc. Some vibration exciters need a ground support to which the actuator must be fixed, as in this case represented in Figure 2, where a hydraulic cylinder is adopted to excite a bridge. In this case, the distance between the ground and the bridge is covered by a truss. In some cases, the ground support is not available (as, for example, if the distance between the ground and the bridge is very large) and other type of exciters must be used such as counter-rotating discs supporting eccentric masses to generate a harmonic unidirectional force (Figure 3a). Such devices were widely used in the 1960s to excite structures for seismic tests [15,16]. In the same era, exciters based on reciprocating compressed air engines or internal combustion engines (Figure 3b), as well as some with a mass moved by a hydraulic actuator (Figure 4), were developed. Nowadays, commercial exciters, constituted by a mass that is driven to move in a reciprocating way, are available [17] and able to operate in the low frequency range 0.5–20 Hz; to exert a sufficiently high force, the masses are forced to perform reciprocating motions characterized by long strokes.

c. The environmental excitation consists in detecting small vibrations of the structure due to random excitations generated by artificial sources (road or railway traffic, industrial plant, etc.) or by natural sources (wind, seismic microtremor, etc.). In this case, the analysis adopted to identify the structure modal parameters is known as *operational modal analysis* (OMA) or as *ambient modal identification* [18,19]. This is a promising technique since it does not require the use of a vibration exciter and the corresponding expenses; for example, if the structure is sufficiently deformable, the wind acting on it could be sufficient to generate a stochastic action, similar to white noise. Such tests could also be carried out under normal operating conditions if the mass of the pay load is small compared to that of the structure and negligibly influences the natural modes of the structure.

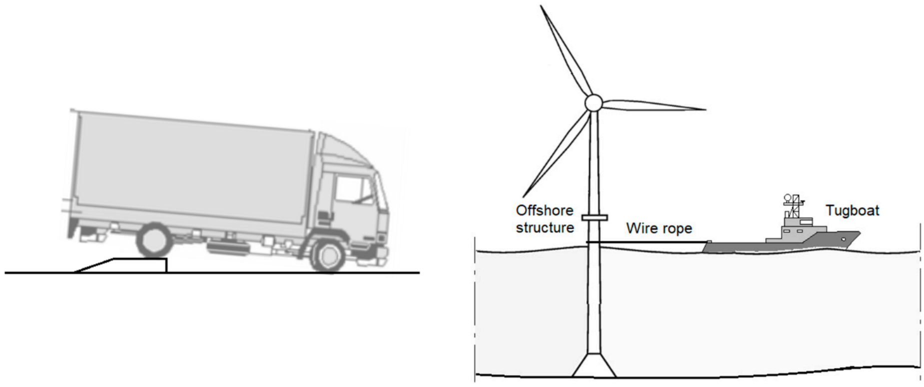

(**a**) (**b**)

Figure 1. Examples of free response of the structure due to (**a**) truck going down a step to excite a bridge, (**b**) load applied to an offshore structure suddenly released.

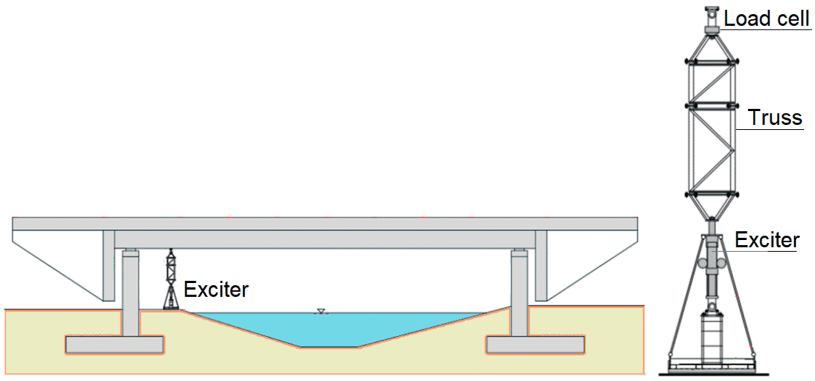

Figure 2. Bridge excited by a hydraulic cylinder fixed on the ground.

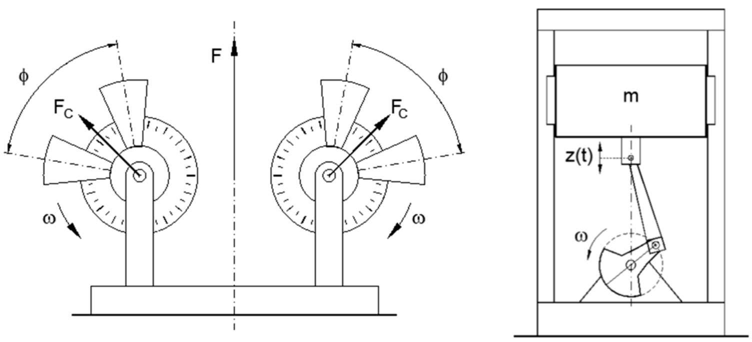

(**a**) (**b**)

Figure 3. Vibration exciters: (**a**) counter-rotating discs supporting eccentric masses; (**b**) reciprocating engine.

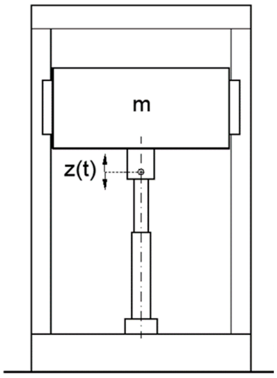

Figure 4. Reaction mass vibration exciters.

These analyses have the drawback of exciting vibrations of small amplitude and for this reason, some parameters cannot be estimated correctly, such as, for example, the damping ratios that are amplitude dependent. Furthermore, considering that this technique requires a greater expertise, laboratories performing monitoring tests often prefer to adopt vibration exciters which involve easier data processing.

Tests conducted using impulsive excitation have been used in mechanical engineering for many years. Instrumented hammers are also used for testing large structures [20]. The hammer test is a quick and accurate way to determine the dynamic characteristics of the structure although the mass of the hammer must increase as the size of the structure increases with the risk of locally damaging the impact zone when high levels of force are applied. The choice between a reaction mass system and a loading hammer depends on the objective of the test: shakers are used when it is desired to apply a controlled vibration with specific frequencies while the loading hammer is used to evaluate the frequency response of the structure.

This paper investigates the possibility of adopting a vibration exciter consisting of an electrodynamic shaker whose spring is constituted by an air spring so that, by appropriately adjusting the pressure of the spring, it is possible to modify its natural frequency to make it equal to the excitation frequency in order to amplify the transmitted force. In this way, the force required to drive the mass is small, as it must be equal to the viscous rection, while the transmitted force is high as it is equal to the vectorial sum of the stiffness and damping reactions [21]. Furthermore, the power required to drive the mass is very low, similar to what happens for devices like integrated gyroscopes [22] or Coriolis mass flowmeters [23]. It is possible to modify the air spring stiffness by adjusting the air mass to inflate or deflate the spring [24]. Thus, by continuously changing the natural frequency of the vibrating system and adapting the forcing frequency, accordingly the excitation frequency, it is possible to perform a frequency sweep test on the structure under test. In general, this type of exciter can also be used to generate controlled vibrations in other types of structures for which, for example, certification tests are required [25].

In the paper, after the description of the proposed exciter, the results of some preliminary experimental tests are reported to evaluate the positive aspects and the drawbacks of this type of exciter.

2. Vibration Exciters

To excite a large structure to vibrate along the vertical direction, since it is generally impossible to apply a force through an actuator due to the difficulty of having an efficient ground support, the following exciters can be adopted.

2.1. Counter-Rotating Discs Supporting Eccentric Masses

The exciter is composed of two counter-rotating discs (Figure 5a), each supporting two eccentric masses whose relative angular position ψ can be modified to adjust the resultant centrifugal force module exerted by each disc; the centrifugal force is zero if ψ is equal to 180° (Figure 5a) and it is maximum if the two masses are in phase ($\psi = 0$) (Figure 5b).

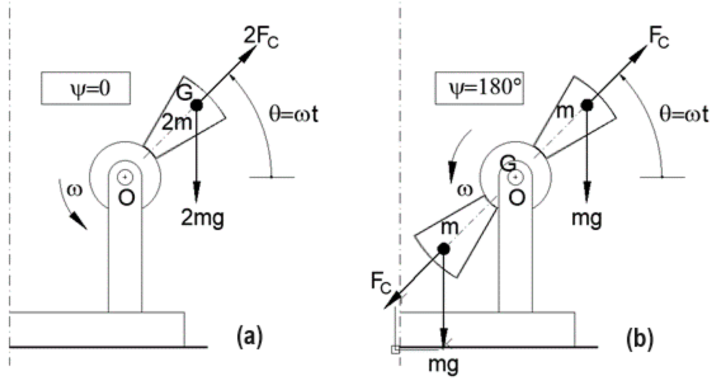

Figure 5. Counter-rotating discs: (**a**) ψ = 0; (**b**) ψ = 180°.

The masses on the two discs are arranged to generate a unidirectional harmonic force F along the vertical direction, the horizontal components of the centrifugal forces being balanced. The vertical component of force F depends on the eccentricity e of the center of mass with respect to the rotation axis (passing through the geometric center of the disk) and on the square of the rotation speed. Indicating with r the distance of the center of mass of each mass, the disc eccentricity is equal to the following:

$$e = rcos(\psi/2) \tag{1}$$

Therefore, the vertical force transmitted to the structure under test depends on the rotating speed and on the angle ψ defined by the eccentric masses angular relative position (Figure 6):

$$F = 2F_c\, sin(\omega t) = \left[4m\omega^2 rcos(\psi/2)\right] \cdot sin(\omega t) \tag{2}$$

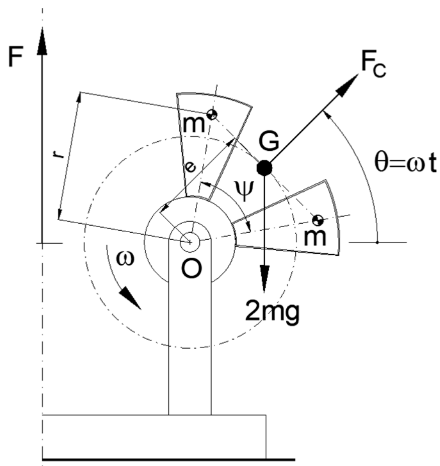

Figure 6. Rotating disc supporting two eccentric masses.

For the synthesis of the device, it is necessary to establish the magnitude of the excitation force F which must be able to excite a measurable forced vibration possibly quite constant as the excitation frequency varies. Therefore, to define the static moment (mr) of the eccentric masses, it is assumed that the angle ψ is zero in correspondence with the lowest frequency of the range to be investigated. From Equation (2):

$$mr = \frac{F}{4\omega^2} \tag{3}$$

Then, for growing values of the forcing circular frequency ω, angle ψ assumes the following value:

$$\psi = 2arccos\left(\frac{F}{4mr\omega^2}\right) \quad (4)$$

Finally, for each value of ψ, the eccentricity e of the rotor is defined by Equation (1) and the power required to drive the two rotors at the rotating speed ω, can be defined as below:

$$P_m = 4mge\omega\ cos\omega t \quad (5)$$

Figure 7 reports the ψ angle and the power required to drive the device, so as to deliver a 2500 N magnitude force if the minimum excitation frequency is 1 Hz, vs. rotational speed (circular frequency) and the mass of each disc is characterized by a mass of 80 kg with an eccentricity of 0.2 m. The diagram shows that for increasing rotational speed, the power to be supplied decreases as the eccentric masses of each rotor tend to be arranged in counterphase with e tending to zero.

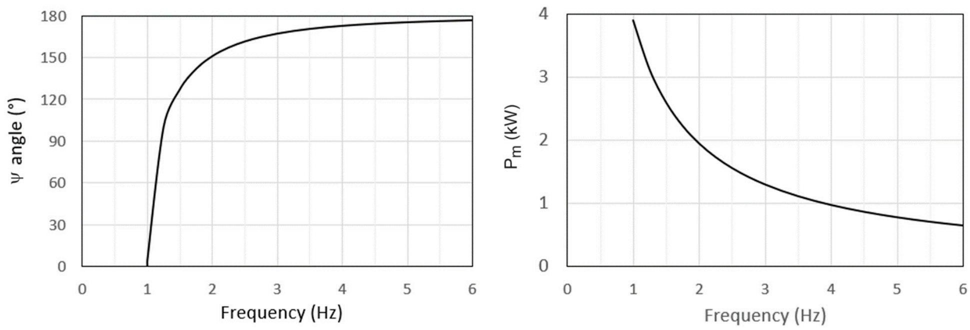

Figure 7. Angle ψ and power required to excite the structure with a constant magnitude force.

2.2. Reaction Mass System

This kind of exciter consists of a mass to which a periodic movement is imposed by means of a slider–crank mechanism (Figure 8a) or by a linear actuator (Figure 8b). The mechanism may be driven by the pressure force acting on mass m that can be seen as the piston of a reciprocating compressed air engine or of an internal combustion engine; furthermore, the mechanism may be driven by an electric motor acting on the crank. In addition, to generating a reciprocating excitation force, the slider–crank mechanism generates a periodically variable component of lateral force that can be avoided by adopting a couple of a counter-rotating connecting rod-crank mechanism acting on the same mass which, however, increases the complexity of the device.

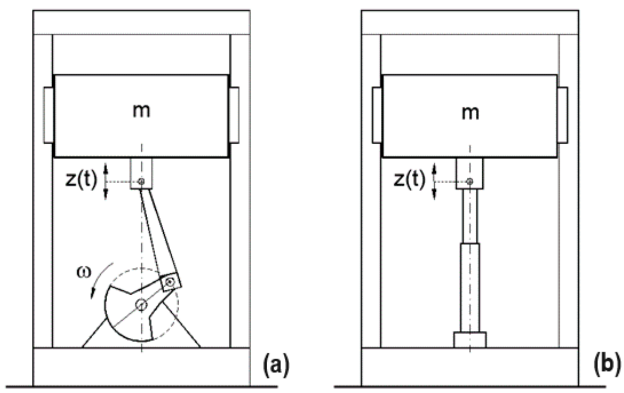

Figure 8. Mass forced to perform a reciprocating motion by means of (**a**) a slider–crank mechanism, (**b**) a linear actuator.

With reference to a linear actuator (Figure 8b), the driving force required to drive the mass m along the vertical direction with a reciprocating law is as follows:

$$F_d(t) = mg + F = mg + m\ddot{z} \tag{6}$$

If a harmonic motion, $z(t) = Z\ sin\omega t$, with amplitude Z and circular frequency ω is assigned to the mass m, to generate an inertia force F of assigned magnitude, the motion amplitude will depend on the circular frequency:

$$Z = \frac{F}{m\omega^2} \tag{7}$$

The power required to drive the device is the following:

$$\begin{aligned} P_m(t) = F_d \cdot \dot{z} = \left(mg - m\omega^2 Z\ sin\omega t\right) \cdot Z\omega\ cos\omega t = \\ = mgZ\omega\ cos\omega t - \frac{mZ^2\omega^3}{2}\ sin2\omega t = P_1(t) - P_2(t) \end{aligned} \tag{8}$$

Figure 9 shows the power required to perform a load-cycle for a 2500 N force magnitude and a forcing frequency of 1 Hz (in the figure $\theta = \omega t$). Figure 10 shows the motion amplitude and the required power versus the forcing frequency. It is evident that at low frequency a long stroke movement is required.

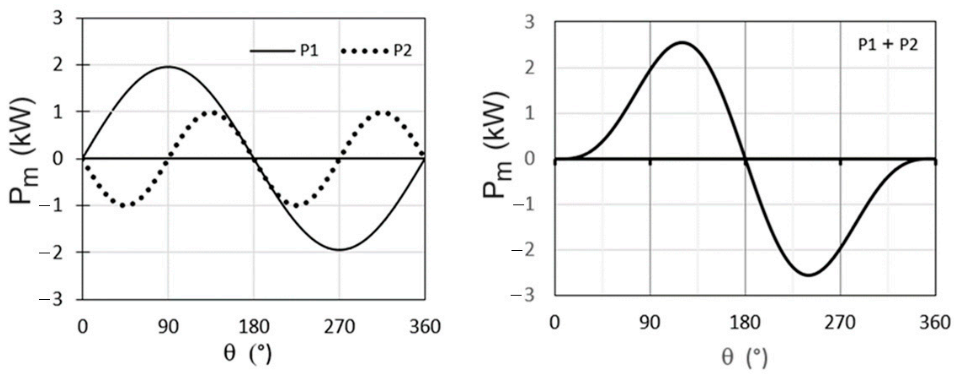

Figure 9. Power required for m = 250 kg and f = 1 Hz.

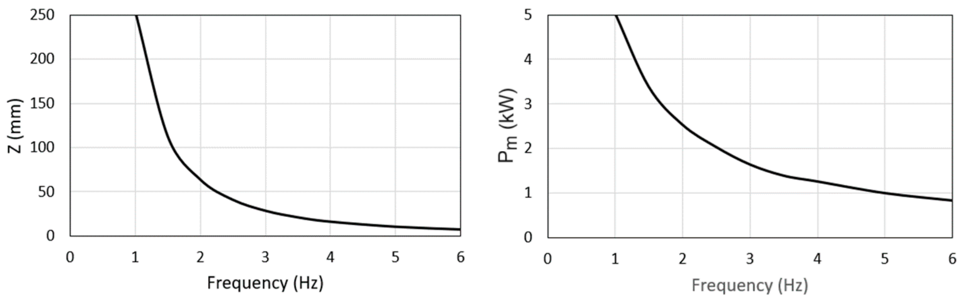

Figure 10. Motion amplitude and power vs. frequency to excite the structure with a constant magnitude force.

In [26], the possibility of using an array of small dynamic exciters for forced vibration tests of short and medium span bridges is proposed. In particular, the possibility of adopting devices used in home theatre applications to shake the floor and furniture to provide tactile sensations to viewers is evaluated.

Finally, it would be possible to move the reaction mass using an electrodynamic shaker [27,28] which is a device normally used for controlled and reproducible vibration tests. This type of shaker is known for its energy efficiency and for generating strong vibrational accelerations. The mobile part of the shaker, sustained by springs, is connected to a coil immersed in a magnetic field which is powered by a signal generator and an amplifier. As the frequency of the current varies, the mobile part behaves like a vibrating system with one degree of freedom and therefore, far from resonance conditions, the force transmitted to the base of the device is small.

Vibration exciters, both with rotating masses and with translating masses, are mainly distinguished by the range of excitable frequencies, the size, the mechanical complexity, and the control system that manages the motors that drive the moving masses. It is not easy to make a direct comparison between the various types of exciters, since the performances, in terms of effective power, depend on the chain of machines that define the entire device such as, for example, the presence of an electric motor with reduction gear for the counter-rotating discs, or of a pump with hydraulic cylinder for an exciter with a reaction mass with linear actuator.

3. Vibration Exciter Based on the Use of an Air Spring

In this paper, the possibility of adopting an electrodynamic shaker, whose reaction mass is suspended on an air spring so that its stiffness can be adjusted by means of the inflating pressure, was evaluated. Figure 11 shows the scheme of the exciter which is made up of a mass suspended on an air spring and is excited to vibrate by a coil like that of electrodynamic exciters. The behavior of the air spring, which characterizes the novelty of the proposal, is characterized below, neglecting the presence of the coil.

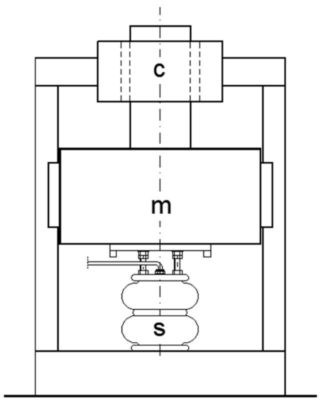

Figure 11. Vibration exciter (s = air spring; m = reaction mass; c = coil).

The linear elastic theory of a one degree of freedom vibrating system (Figure 12) shows that, if the mass is excited to vibrate by a harmonic force $F(t)$, with magnitude F_0 and circular frequency ω equal to the natural circular frequency, the force F_T transmitted to the suspension support is considerably amplified with respect to the forcing one. In this condition, the force required to drive the mass is small. In fact, in steady state condition, the driving force must be equal to the viscous rection, while the transmitted force is high as it is equal to the vectorial sum of the stiffness and damping reactions, as highlighted by phasors represented in Figure 12b,c. In the same figure, m, k, σ are the mass, the stiffness, and the damping of the vibrating system while ϕ is the phase delay. Even in transients, such as for example in the start-up phase, the forcing action may have a lower intensity than that necessary to lift the mass, thanks to the resonance condition.

The adoption of an air spring allows the stiffness k to be changed by adjusting the pressure of the air spring. In this way it is possible to change the natural frequency of the vibrating system by inflating or deflating the spring; so, by changing accordingly the excitation frequency, it is possible to transmit an amplified force to the suspension support at different frequencies so that the system could be adopted as a vibration exciter.

At resonance frequency, the power required to excite a harmonic motion is as follows:

$$P_m(t) = \sigma \dot{z}^2 = \frac{\sigma\omega^2 Z^2}{2} + \frac{\sigma\omega^2 Z^2}{2} cos2\omega t \tag{9}$$

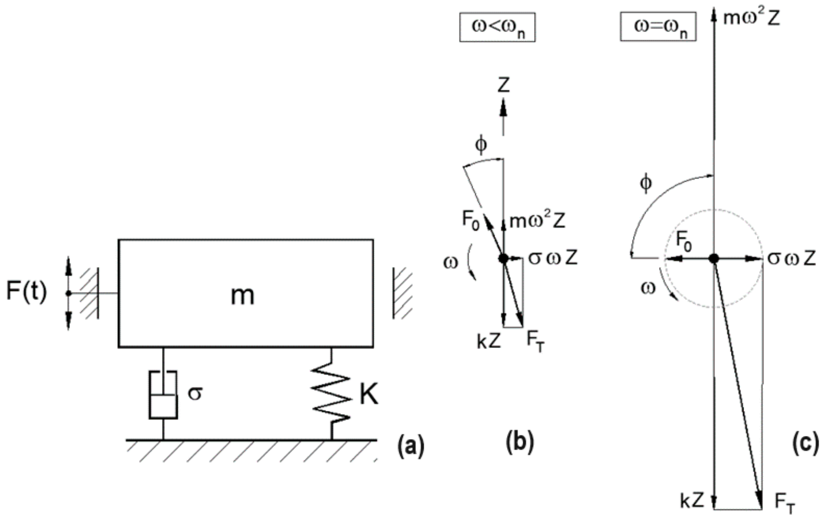

Figure 12. One degree of freedom vibrating system: (**a**) scheme; (**b**) transmitted force for $\omega < \omega_n$; (**c**) transmitted force in resonance condition ($\omega < \omega_n$).

For small damping coefficient σ the power required to excite the movement is very small while the transmissibility ($T = F_T/F_0$) can reach high values. The transmitted force is equal to the following:

$$F_T = \sqrt{(kZ)^2 + (\sigma\omega Z)^2} = F_0 \frac{\sqrt{1 + \left(2\frac{\sigma}{\sigma_c}\frac{\omega}{\omega n}\right)^2}}{\sqrt{\left(1 - \frac{\omega^2}{\omega_n{}^2}\right)^2 + \left(2\frac{\sigma}{\sigma_c}\frac{\omega}{\omega n}\right)^2}} \tag{10}$$

$\omega_n = \sqrt{\frac{k}{m}}$ being the circular natural frequency and $\sigma_c = 2\sqrt{km}$ the critical damping.

The air spring allows the stiffness of the system to be modified, thus allowing a range of frequencies that can be excited in resonance to be identified. Figure 13 reports the transmissibility trend vs. the forcing frequency for F_0 = 1 N. The diagram is plotted for different values of the spring stiffness and therefore for different values of the system natural frequency; each curve is plotted for two values of the damping ratio. Figure 13 qualitatively shows that the transmissibility is maximum in resonance conditions and that its peak value depends on the damping.

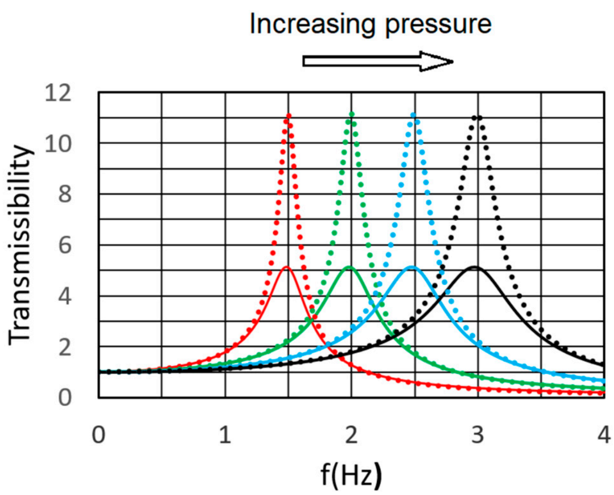

Figure 13. Transmissibility for different stiffness values of the spring and for two values of the damping ratio σ/σ_c (0.1 for continuous lines; 0.05 for dotted lines).

4. Air Spring Model

The air spring is difficult to model as its stiffness and damping characteristics depend on the air transformation and on the rubber envelope characteristics. A first approximation model is the *classical model* [29] based on the piston-cylinder scheme (Figure 14a). The air pressure p is defined considering a polytropic transformation due to the volume variation V. Indicating with V_0 and p_0 the initial volume and pressure, respectively, the pressure assumes the following expression: $p = p_0(V_0/V)^\gamma$ γ being the exponent of the polytropic transformation equal to 1.41 for adiabatic transformation (rapid variation of the volume for which it is possible to neglect heat exchanges with the environment). For this application the exponent of the polytropic can be properly chosen as equal to 1.38; this value is normally adopted for air springs used as vibration isolators.

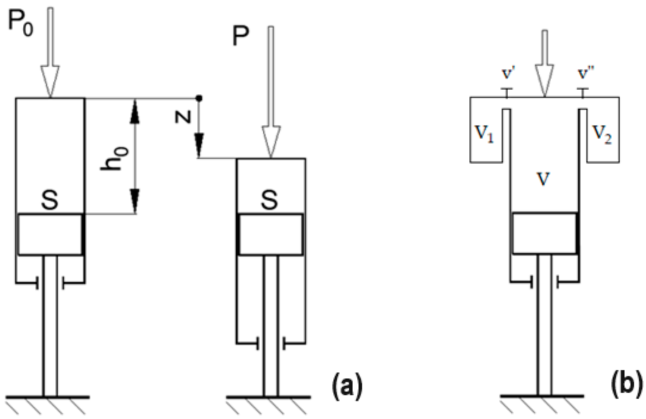

Figure 14. Simple air spring: (**a**) air spring deflection under load; (**b**) air spring with auxiliary volume.

With reference to the scheme of Figure 14a, the expression of the pressure can be deduced from the following expression:

$$P = P_0\left(\frac{V_0}{V}\right)^\gamma = P_0\left(\frac{h_0}{h_0 - z}\right)^\gamma = P_0\left(\frac{1}{1 - z/h_0}\right)^\gamma \tag{11}$$

$P = pS$ being the load acting on the spring and $h_0 = h + z$ the initial air spring height. The spring stiffness and the natural frequency of the system can be obtained by deriving Equation (13) with respect to z:

$$k_z = \frac{dP}{dz} = \frac{\gamma\, P_0}{h_0}\frac{1}{(1 - z/h_0)^{\gamma+1}} = \frac{\gamma\, P}{h_0 - z} = \frac{\gamma\, mg}{h_0 - z} \tag{12}$$

Therefore, the natural frequency is as follows:

$$f_z = \frac{1}{2\pi}\sqrt{\frac{k_z}{m}} = \frac{1}{2\pi}\sqrt{\frac{\gamma\, g}{h_0 - z}} \tag{13}$$

Considering that: $p = P/S$; $h_o = V/S$, the spring stiffness can be expressed as a function of the area S:

$$k_z = \frac{\gamma\, P}{h_0 - z} = \frac{\gamma\, pS}{\frac{V}{S} - z} = \frac{\gamma\, pS^2}{V - zS} \tag{14}$$

The natural circular frequency of the vibrating system varies with the spring height z, depending on the weight of the suspended mass m. Equation (14) shows that it is possible to reduce the stiffness of the spring by increasing the air volume V. To this end it is possible to connect the spring with one or more auxiliary volumes of suitable capacity (Figure 14b). These capacities can be equipped with valves (v′ and v′′ in Figure 14b) to adjust the air volume of the spring.

Air springs are generally made up of a fiber-reinforced elastomeric envelope; therefore, unlike the simple air spring, the cross-section area S is not constant but depends on the operating condition. In this case, the *effective area* (S_{eff}) on which the air pressure acts is defined as the ratio between the applied force and the pressure ($S_{eff} = P/p$) and its trend vs. load depends on the air spring type; for the lobe spring it increases with the load, as qualitatively represented in Figure 15.

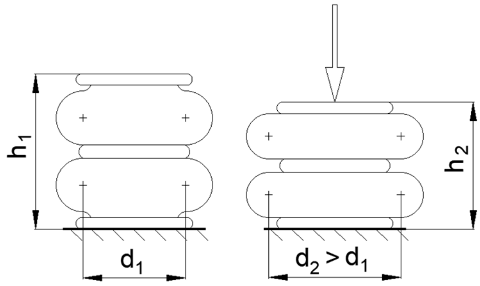

Figure 15. Qualitative variation under load of the spring effective area.

A theoretical evaluation of the stiffness of convoluted air springs, which takes into account the number of lobes, is reported in [30].

5. Experimental Investigation

In the following, the results of two kinds of experimental tests are reported. The first set of tests had the aim of evaluating the range of possible values of the air spring stiffness and therefore the obtainable range of the natural frequency, while the second kind of tests were performed to estimate the damping of the system in different operating conditions. Both tests were performed adopting a double convoluted air spring (the model adopted for the tests is the commercial air spring Firestone mod.25).

5.1. Static Tests

To evaluate the spring stiffness, static tests were carried out by connecting the spring to an auxiliar tank. The connection is equipped with a valve that can be set in an open or closed way (Figure 16a). By loading the spring with a press, the force–displacement diagrams were obtained starting from different initial air pressure.

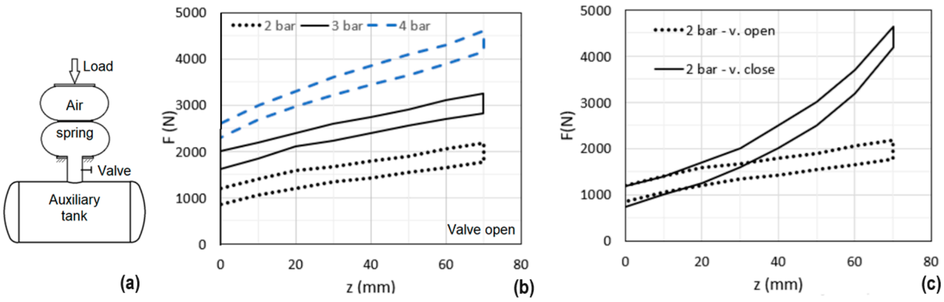

Figure 16. Force–displacement diagrams: (**a**) Scheme of the connection between spring and tankvalve open; (**b**) comparison for different initial pressure; (**c**) comparison between open and closed valve.

By opening the valve, the diagrams exhibit an almost linear trend (Figure 16b); therefore, the stiffness is quite constant with the spring deflection z. By closing the valve, the force grows more rapidly as shown in Figure 16c, which reports a comparison with the open valve case, for the initial pressure of 2 bar. When the valve is closed, due to the lower volume, the air pressure grows more rapidly as shown by Equation (14); in fact, as the height z of the spring decreases, the denominator of Equation (14) is reduced and the effective area S that appears in the numerator increases.

For the initial pressure of 2 bar, the comparison between the stiffness trend versus the spring deflection is reported in Figure 17a for the open and closed valve, while the corresponding trend of the natural frequency versus the spring deflection is shown in Figure 17b.

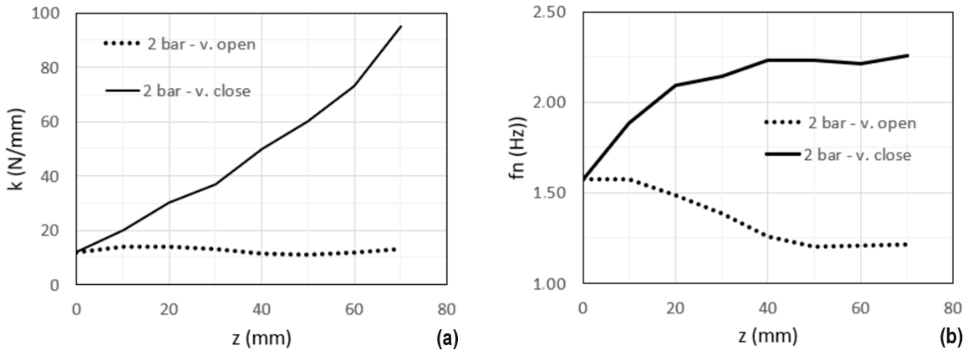

Figure 17. Initial pressure of 2 bar: (**a**) stiffness vs. deflection; (**b**) natural frequency trend vs. deflection.

So, it would be possible to adopt a tank with an adjustable volume, to change the natural frequency in the range included between the two curves.

5.2. Dynamic Tests

Several tests were carried out by means of the test rig, schematized in Figure 18, consisting of a mass suspended on the same air spring. The mass is constituted by several steel discs fixed on a support that is constrained to move along the vertical direction by means of a recirculating ball linear guide. The vertical position of the sliding support is measured by the laser displacement sensor $\mu\varepsilon$ − optoNCDT 1420 (FS = 50 mm; linearity = ± 0.08%FS; repeatability 2 µm), FS being the full scale defining the maximum range the sensor can measure. The load acting on the air spring is measured by the washer type load cell Futek LTH300 (FS = 4448 N = 1000 lbf; linearity = ± 0.5%FS; repeatability ± 0.5%FS).

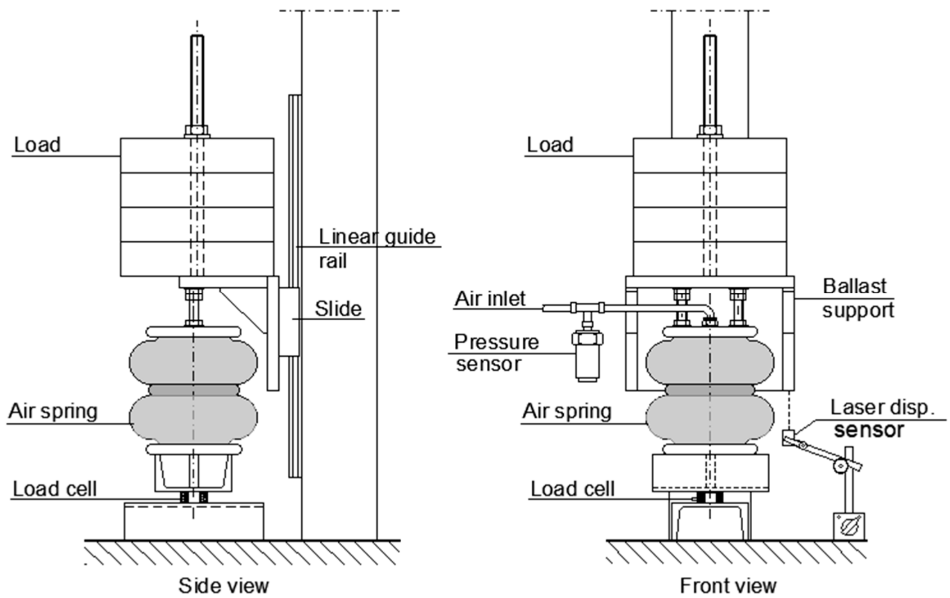

Figure 18. Scheme of the test rig for dynamic tests.

The spring is connected to an air compressor (36 L/min @ 0 bar; p_{max} = 9 bar). The pressure is measured by means of a pressure gauge and the pressure sensor Parkers PTDVB0251B1C2 (FS = 25 bar; linearity = ± 0.3% FS; repeatability ± 0.22% FS). Figure 19 reports the photo of the test rig; at the present, it allows a suspended mass of about 70 kg to be adopted. This load is small in comparison to the spring characteristics and therefore, the maximum air pressure can be equal to 4 bar while the spring could work up to 8 bar. With the constant weight *P* due to the suspended mass, the spring deflection was detected for different values of the air pressure p (Figure 20a); for each operating condition, the effective area ($S_{eff} = P/p$) of the spring was deduced (Figure 20b).

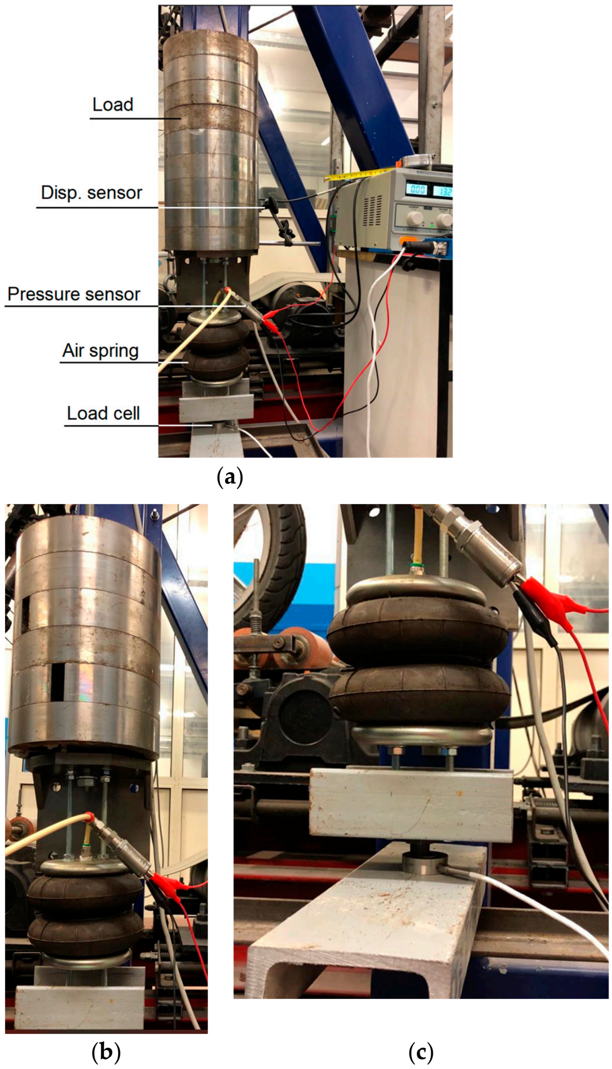

Figure 19. Photos of the test rig (**a**) general view; (**b**) particular of the ballast on the spring; (**c**) particular of the load cell under the spring.

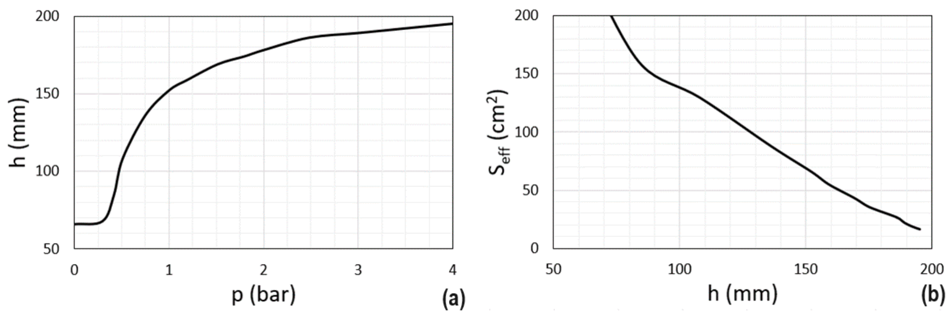

Figure 20. (**a**) Air spring height vs. pressure for a constant load of 660 N; (**b**) Effective area vs. height.

The suspended mass was excited to perform free vibrations (Figure 21), starting from different operating conditions (air pressure and spring height). The motion of the mass was detected together with the pressure variation and the force exchanged with the ground. From the displacement diagram, the natural frequency (f_n), the damping ratio (σ/σ_c), and the transmissibility (T) were estimated. The test was repeated for different values of the initial pressure in the range 0.5–4.0 bar to plot the trend of f_n, σ/σ_c and T (Figure 22). Such diagrams show that, by increasing the pressure the following occur:

- the natural frequency increases;
- the damping ratio assumes the trend reported in Figure 22b. This trend can be explained by considering that the damping is due to the hysteretic dissipative actions of the elastomeric envelope of the spring and the friction in the guide of the suspended mass. Furthermore, when the spring is highly compressed, the dissipative actions are also due to the friction forces that arise in the contact between the lobes of the spring. For this reason, as the pressure increases, the damping initially decreases rapidly (since the lobes move away from each other) and then it increases slightly;
- the transmissibility is greater than 10 where the damping ratio reaches lower values.

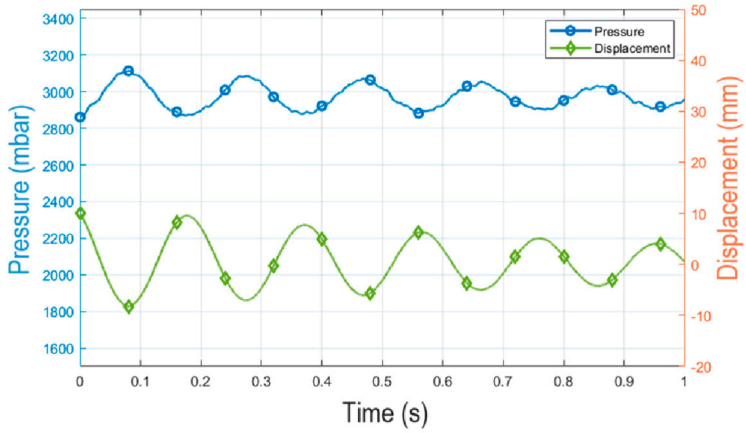

Figure 21. Suspended mass free vibrations for p = 3 bar (sampling frequency of 1 kHz).

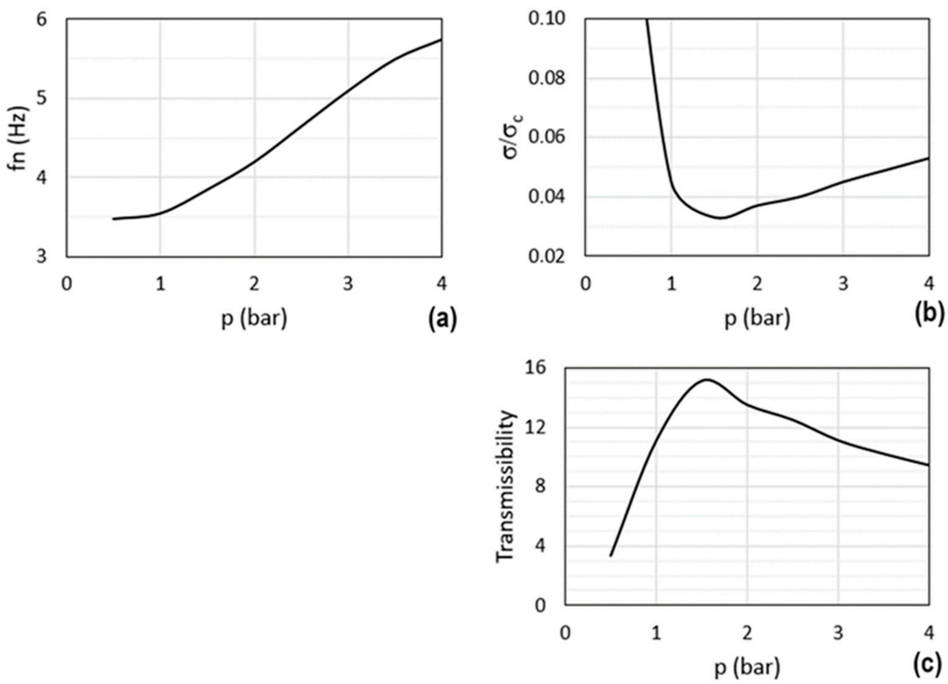

Figure 22. Suspended mass free vibrations for initial pressure of 3 bar. (**a**) Natural frequency; (**b**) damping ratio; (**c**) transmissibility.

6. Numerical Investigation

The vibrating system can be schematized as a single degree of freedom system in which the parameters depend on the inflation pressure of the spring and, therefore, on the initial configuration of the spring. For each pressure value it is possible to define the height at which static equilibrium is achieved; around this position it is possible to assume that the stiffness and damping parameters are constant, and it is possible to define the natural frequency of the system. By forcing the system to vibrate with the same frequency, thanks to the resonance, the action transmitted to the spring support is amplified.

To perform some of the numerical simulations, the stiffness and damping of the system were expressed as a function of the air pressure by means of a sixth-degree polynomial, interpolating the experimental data reported in Figure 22. The simulation results highlighted that, if the spring pressure is changed slowly and the forcing frequency is simultaneously adjusted so that the system is kept in a resonant condition, the transmitted force is always amplified; the amplification is greater when the damping coefficient takes on smaller values.

Figure 23 shows the trend of the force transmitted to the support of the spring vs. frequency excitation. The black curve was obtained by integrating the equation of motion of the vibrating system, slowly varying the excitation frequency (0.001 Hz/s) and continuously adapting the air spring stiffness and damping values so that the system was always in resonance conditions. This curve turns out to be quite the envelope of the frequency responses of different vibrating systems, each characterized by constant stiffness and damping parameters, defined as a function of the pressure of the air spring.

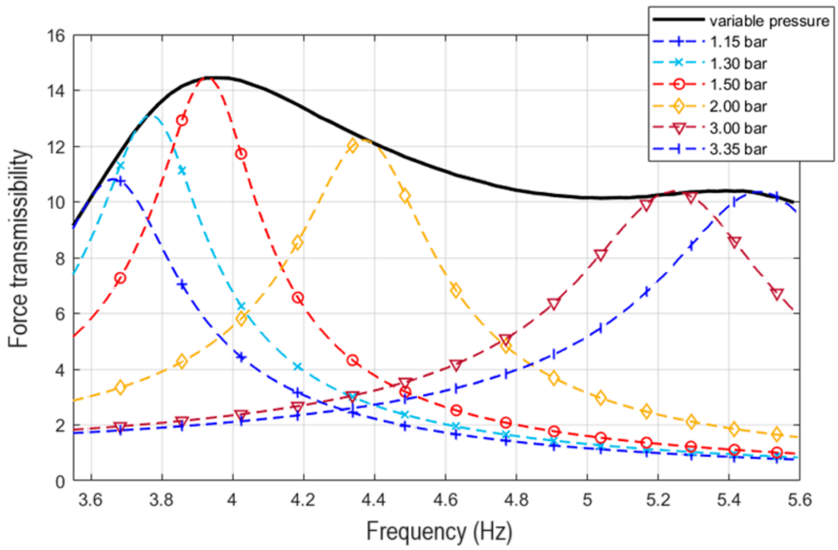

Figure 23. Continuous variation of pressure and of frequency excitation to maintain the vibrating system in resonant condition.

The dynamic response of the structure should be affected by the presence of the air spring shaker. However, due to the differences in mass and stiffness between the shaker and the structure, it is possible to assume that the structure dynamics are not significantly influenced by the presence of the air spring shaker. This is evidenced by the first approximation two degrees of freedom vibrating model (Figure 24), in which the shaker is represented by the subsystem with parameters m_1, k_1, σ_1, and the structure with parameters m_2, k_2, σ_2. Figure 25 shows the trend of the force transmitted by the exciter to the structure. This force is given by the sum of the forces exerted by the coil and by the air spring depending on the relative motion of the two masses. Each curve was obtained for different values of the spring stiffness k_1 (air spring), according to the frequency excitation; for simplicity the damping was kept constant (σ_1 = 130 Ns/m). The diagrams were generated adopting the following parameters: m_1 = 63 kg, m_2 = 320,000 kg, k_2 = 200e6 N/m. The natural frequency of the subsystem structure is about 4 Hz. The amplitude of the harmonic forcing action was selected to be 1 N. The diagram shows that the exciter, if adopted in resonance conditions, exerts on the structure an amplified force compared to that provided by the coil. The slight influence due to dynamic coupling of the system is evidenced by the shape of the curve at 40 N/mm.

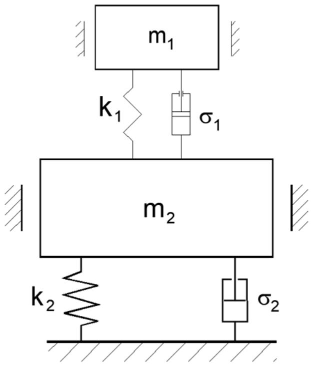

Figure 24. Two degree of freedom system.

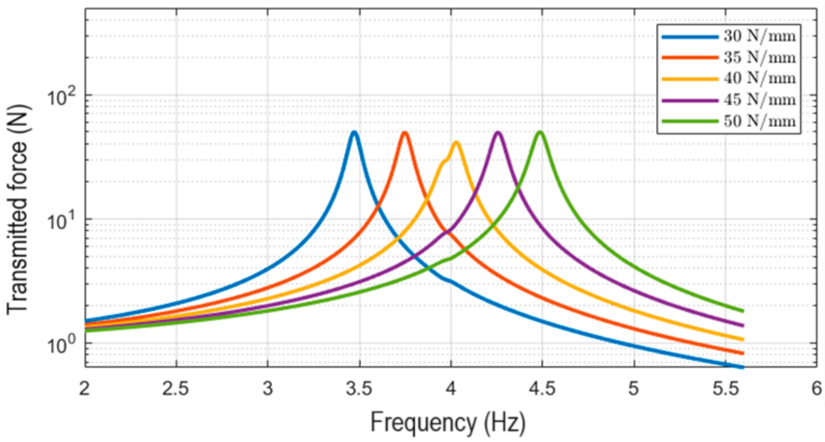

Figure 25. Transmitted force vs. frequency for different values of the air spring stiffness.

7. Conclusions

In this paper, the possibility of using a vibration exciter for large structures consisting of a mass suspended on an air spring and forced to vibrate in resonance condition, was explored. This type of exciter would have the advantage of amplifying the force transmitted to the structure and of being constructively simple to manufacture as it is made up of components produced in large series.

Some preliminary tests were carried out to estimate the characteristic parameters of an air spring as the pressure varies. The test results were used to carry out several numerical simulations.

However, the tests were carried out with a small sprung mass compared to the characteristics of the air spring used. Due to this limitation, it was not possible to explore the full range of pressures applicable to the adopted spring. As a result, the exciter has a narrow range of frequencies that can be excited.

To widen the frequency range, it is necessary to combine suitably the suspended mass with the characteristics of the spring and to adopt a spring with a greater stroke. Furthermore, it would also be possible to use a different type of air spring such as, for example, a rolling air spring which could be suitably designed to have a high variation of effective area with spring travel and capable of realizing greater variation of stiffness of the system as the height of the spring varies. Through static experimental tests it was shown that it is also possible to increase the range of excitable frequencies by connecting (or disconnecting) the spring with one or more air tanks.

The dynamic coupling of the shaker with the structure was considered using a first approximation model with two degrees of freedom; the model highlighted that, due to the large difference in the mass and stiffness of the two subsystems, this coupling does not markedly influence the dynamic response of the structure and confirmed the amplification of the force transmitted to the structure.

Author Contributions: Conceptualization, S.P. and G.D.M.; methodology, S.P. and E.R.; software, R.B.; validation, R.B. and D.D.F.; formal analysis, R.B. and E.R.; investigation, G.D.M. and S.P.; writing—original draft preparation, S.P. and E.R.; writing—review and editing, R.B., D.D.F., G.D.M., S.P. and E.R.; supervision, R.B., D.D.F., G.D.M., S.P. and E.R. All authors have read and agreed to the published version of the manuscript.

Funding: This research received no external funding.

Data Availability Statement: Data are reported in the text; developed software is available on request.

Acknowledgments: The authors are grateful to Rosario Moreschi and Gennaro Stingo for their collaboration during the laboratory tests.

Conflicts of Interest: The authors declare no conflict of interest.

Abbreviations

e	eccentricity of the centre of mass of the rotating disc
f	frequency
f_n	natural frequency
F	vertical component of the inertia force
F_C	centrifugal force magnitude
F_d	driving force magnitude
F_0	exciting force magnitude
F_T	transmitted force
g	gravity acceleration
h	spring height
h_0	initial spring height
k	stiffness
m	moving mass
p	pressure
p_0	initial pressure
P	load acting on the spring
P_0	initial load acting on the spring
P_m	driving power
r	eccentricity of the centre of mass of each rotating mass
S	air spring cross section area
S_{eff}	air spring effective area
V	volume
V_0	initial volume
z	moving mass vertical displacement
Z	amplitude of the vertical motion of the moving mass
γ	exponent of the polytropic transformation
θ	angular rotation
σ	damping coefficient
σ_{cr}	critical damping
ϕ	phase delay
ψ	eccentric masses angular relative position
ω	forcing circular frequency
ω_n	natural circular frequency

References

1. Fujino, Y.; Siringoringo, D.M.; Ikeda, Y.; Nagayama, T.; Mizutani, T. Research and implementations of structural monitoring for bridges and buildings in Japan. *Engineering* **2019**, *5*, 1093–1119. [CrossRef]
2. Bień, J.; Kużawa, M. Dynamic Tests in Bridge Health Monitoring. *Stud. Geotech. Mech.* **2020**, *42*, 291–296. [CrossRef]

3. Sung, Y.; Lin, T.; Chiu, Y.; Chang, K.; Chen, K.; Chang, C. A bridge safety monitoring system for prestressed composite box-girder bridges with corrugated steel webs based on in-situ loading experiments and a long-term monitoring database. *Eng. Struct.* **2016**, *126*, 571–585. [CrossRef]
4. Mishra, M.; Lourenço, P.B.; Ramana, G.V. Structural health monitoring of civil engineering structures by using the internet of things: A review. *J. Build. Eng.* **2022**, *48*, 103954. [CrossRef]
5. Bonopera, M.; Liao, W.; Perceka, W. Experimental–theoretical investigation of the short-term vibration response of uncracked prestressed concrete members under long-age conditions. *Structures* **2022**, *35*, 260–273. [CrossRef]
6. Peeters, B.; Maeck, J.; De Roeck, G. Vibration-based damage detection in civil engineering: Excitation sources and temperature effects. *Smart Mater. Struct.* **2001**, *10*, 518–527. [CrossRef]
7. ASofi, A.; Regita, J.J.; Rane, B.; Lau, H.H. Structural health monitoring using wireless smart sensor network—An overview. *Mech. Syst. Signal Process* **2022**, *163*, 108113.
8. Brancati, R.; Di Massa, G.; Genovese, A. Experimental Investigation to Enhance Performances of MRE in Energy Harvesting. In *Mechanisms and Machine Science*; Springer: Cham, Switzerland, 2023; Volume 134, pp. 3–10.
9. Niyirora, R.; Ji, W.; Masengesho, E.; Munyaneza, J.; Niyonyungu, F.; Nyirandayisabye, R. Intelligent damage diagnosis in bridges using vibration-based monitoring approaches and machine learning: A systematic review. *Results Eng.* **2022**, *16*, 100761. [CrossRef]
10. Xin, C.; Wang, C.; Xu, Z.; Wang, J.; Yan, S. Damage detection of structures from motion videos using high-spatial-resolution mode shapes and data fusion. *Eng. Fail. Anal.* **2022**, *140*, 106560. [CrossRef]
11. Dong, C.Z.; Catbas, F.N. A review of computer vision–based structural health monitoring at local and global levels. *Struct. Health Monit.* **2021**, *20*, 692–743. [CrossRef]
12. Mangal, L.; Idichandy, V.G.; Ganapathy, C. Structural monitoring of offshore platforms using impulse and relaxation response. *Ocean. Eng.* **2001**, *28*, 689–705. [CrossRef]
13. Cunha, A.; Caetano, E.; Delgado, R. Dynamic Test on Large Cable Stayed Bridge. *J. Bridge Div. Proc. ASCE* **2001**, *6*, 54–62. [CrossRef]
14. Tian, Y.; Zhang, J.; Xia, Q.; Li, P. Flexibility identification and deflection prediction of a three-span concrete box girder bridge using impacting test data. *Eng. Struct.* **2017**, *146*, 158–169. [CrossRef]
15. Hudson, D.E. A New Vibration Exciter for Dynamic Test of Full-Scale Structures, Earthquake Engineering Research Laboratory, 1961, Pasadena, California. Available online: https://authors.library.caltech.edu/26489/1/Hudson_1961.pdf (accessed on 19 September 2023).
16. Jennings, P.C.; Kuroiwa, J.H. Vibration and soil-structure interaction tests nine-story reinforced concrete building. *Bull. Seismol. Soc. Am.* **1968**, *58*, 891–916. [CrossRef]
17. APS Vibration Exciters. Available online: https://www.apsdynamics.com/en/index.html (accessed on 19 September 2023).
18. Ghalishooyan, M.; Shooshtari, A. Operational Modal Analysis Techniques and Their Theoretical and Practical Aspects: A Comprehensive Review and Introduction. In Proceedings of the 5th International Operational Modal Analysis Conference (IOMAC 2015), Gijon, Spain, 12–14 May 2015.
19. Brincker, R.; Zhang, L.; Andersen, P. Modal identification of output-only systems using frequency domain decomposition. *Smart Mater. Struct.* **2001**, *10*, 441. [CrossRef]
20. Maguire, J.R.; Severn, R.T. Assessing the dynamic properties of prototype structures by Hammer Testing. *Proc. Inst. Civ. Eng.* **1987**, *83*, 769–784. [CrossRef]
21. Brancati, R.; De Falco, D.; Di Massa, G.; Pagano, S.; Rocca, E. A Vibration Exciter for Dynamic Testing of Large Structures. In *Mechanisms and Machine Science*; Springer: Cham, Switzerland, 2023; Volume 134, pp. 217–224.
22. Lin, Y.; Qian, W.; Li, H.; Ma, H.; Jin, Z. Resonant micro-optic gyroscope equipped with multi-turn waveguide ring resonator. *Opt. Commun.* **2021**, *491*, 126954. [CrossRef]
23. Adiletta, G.; Cascetta, F.; della Valle, S.; Guido, A.R.; Pagano, S.; Vigo, P. A twin rigid straight pipe Coriolis mass flowmeter. *Measurement* **1993**, *11*, 289–308.
24. Di Massa, G.; Pagano, S.; Strano, S. Cabinet and Shelter Vibration Isolation: Numerical and Experimental Investigation. *Eng. Lett.* **2014**, *22*, 149–157.
25. Luczak, M.M.; Peeters, B.; Manzato, S.; Di Lorenzo, E.; Reck-Nielsen, K.; Berring, P.; Haselbach, P.U.; Branner, K. Research sized wind turbine blade modal tests: Comparison of the impact excitation with shaker excitation. *J. Phys. Conf. Ser.* **2018**, *1102*, 012022. [CrossRef]
26. Grimmelsman, K.A.; Fernstrom, E.V.; Carreiro, J.L. Evaluating Economical Dynamic Exciters for Bridge Vibration Testing. *Sound Vib.* **2014**, *39*, 11–16.
27. Lang, G.F.; Snyder, D. Understanding the Physics of Electrodynamic Shaker Performance. *Sound Vib.* **2001**, *35*, 24–33.
28. Chlebo, O.; Sivý, M.; Musil, M.; Čekan, M. Design of the uniaxial shaker with variable stiffness. *MATEC Web Conf.* **2017**, *107*, 59. [CrossRef]
29. Harris, C.M.; Piersol, A.G. *Harris' Shock and Vibration Handbook*, 5th ed.; McGraw-Hill: New York, NY, USA, 2002.
30. Zheng, Y.; Shangguan, W.B.; Rakheja, S. Modeling and performance analysis of convoluted air springs as a function of the number of bellows. *Mech. Syst. Signal Process.* **2021**, *159*, 107858. [CrossRef]